

A Effect of Elevator Deflection on Lift Coefficient Increment

S.Ravikanth¹, KalyanDagamoori², M.SaiDheeraj³, V.V.S.Nikhil Bharadwaj⁴, SumamaYaqub Ali⁵,
HarikaMunagapati⁶, Laskara Farooq⁷, Aishwarya Ramesh⁸, SowmyaMathukumalli⁹

¹ Assistant Professor , Department Of Aeronautical Engineering, MLR Institute Of Technology,
DundigalHyderabad. INDIA .

^{4,6,8,9} Student , Department Of Aeronautical Engineering , MLR Institute Of Technology, Dundigal ,Hyderabad.
INDIA .

^{2,3,5,7} Student , Department Of Aeronautical Engineering , MLR Institute Of Technology and Management ,
Dundigal ,Hyderabad. INDIA .

ABSTRACT: *Elevators are flight control surfaces, usually at the rear of an aircraft, which control the aircraft's lateral attitude by changing the pitch balance, and so also the angle of attack and the lift of the wing. The elevators are usually hinged to a fixed or adjustable rear surface, making as a whole a tailplane or horizontal stabilizer. The effect on lift coefficient due to an elevator deflection is going to find by assuming the baseline value, initializing the aircraft at a steady state flight condition and then commanding a step elevator deflection. By monitoring the aircraft's altitude and other related measurements, you can record the effect of a step elevator deflection at this flight condition. Repetitions of this experiment with various values will demonstrate how variations in this parameter affect the aircraft's response to elevator deflection. Deflection of the control surface creates an increase or decrease in lift and moment. In this paper we are going to derive the different equations related to the longitudinal stability and control. The design of the horizontal stabilizer and elevator is going to do in CATIA V5 and the analysis is going to perform in ANSYS 12.0 FLUENT.*

Keywords : Horizontal tail , Elevator , CATIA V 5 , CFD Analysis

Cr	=	Root chord
B	=	Half-wing span
λ	=	Quarter chord sweepback angle
AR	=	Aspect ratio
T	=	Taper ratio
Cd	=	Sectional drag coefficient (2D-Airfoil)
Cl	=	Sectional lift coefficient (2D- Airfoil)
CD	=	Drag coefficient (3D-Elevator)
CL	=	Lift coefficient (3D- Elevator)
Cdmin	=	Minimum drag Coefficient
CLmax	=	Maximum lift coefficient
CLmin	=	Minimum lift Coefficient
Cm	=	Pitching moment coefficient
Cmo/4	=	Zero Angle Pitching moment coefficient
CmC	=	pitching moment about the quarter-chord
CL α	=	Lift-Curve slope
L/D	=	Lift-to-Drag Ratio
CG	=	Center of Gravity
t/c	=	Thickness to Chord Ratio
E	=	Young's modulus
G	=	sectional modulus
A	=	Angle Of Attack
PR	=	Poison's Ratio

I. Introduction

Elevators are flight control surfaces, usually at the rear of an aircraft, which control the aircraft's lateral attitude by changing the pitchbalance, and so also the angle of attack and the lift of the wing. The elevators are usually hinged to a fixed or adjustable rear surface, making as a whole a tailplane or horizontal stabilizer. They

may be also the only pitch control surface present, sometimes located at front (early airplanes) or integrated in a rear "all-moving tailplane" also called a slab elevator or stabilator.

The wing into which elevators are hinged (the horizontal stabilizer, usually located at the rear end of an aircraft) has the opposite effect to the main wing. The horizontal stabilizer usually creates a downward force which balances the nose down moment due to the airplane's center of gravity being located in front of the center of lift, and other moments due to the effects of drag and engine thrust.

In trim (balanced) condition, the setting of the elevator determines the airplane's *trim speed* - a given elevator position has only one lift coefficient (and one speed at a given altitude) at which the aircraft will maintain a constant (unaccelerated) condition.

In control mode, the elevators change the aircraft trim and make the aircraft nose-up or nose-down. The elevators decrease or increase the downward force created by the rear wing :

- an increased downward force, produced by *up* elevator, forces the tail down and the nose up. The increased wing angle of attack causes a greater lift to be produced by the wing and more drag, demanding more power to keep the speed or climb,
- a decreased downward force at the tail, produced by *down* elevator, allows the tail to rise and the nose to lower. The decrease in angle of attack reduces the lift, demanding more speed (adding power or going to a descent) to produce the required lift.

Supersonic aircraft have stabilators, because early supersonic flight research revealed that shock waves generated on the rear part of a tailplane rendered hinged elevators ineffective. Delta winged aircraft combine ailerons and elevators – and their respective control inputs – into one control surface, called an elevon.

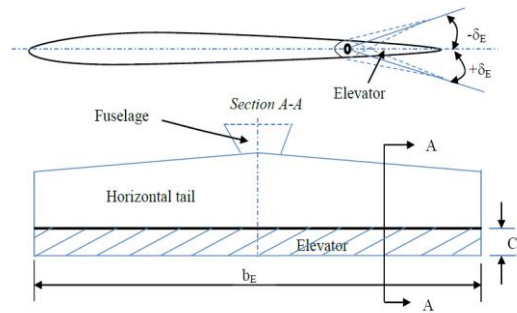
Elevators are usually part of the tail, at the rear of an aircraft. In some aircraft, pitch-control surfaces are in the front, ahead of the wing ; in a two-surface aircraft, this type of configuration is called a canard (the French word for duck) or a tandem wing. The Wright Brothers' early aircraft were of canard type; Mignet Pou-du-Ciel and Rutan Quickie are of tandem type. Some early three surface aircraft had front elevators (Curtiss/AEA June Bug) ; modern three surface aircraft may have both front (canard) and rear elevators (Grumman X-29).

1.2 Objective

The main objective of this project is to study variation of lift, drag and pitching moment coefficient (C_L , C_D and C_m) function of angle of attack and elevator deflection in longitudinal direction.

1.3 Longitudinal stability and control

A very fundamental requirement of a safe flight is longitudinal control; which is assumed to be the primary function of an elevator. An aircraft must be longitudinally controllable, as well as maneuverable within the flight envelope. In a conventional aircraft, the longitudinal control is primarily applied through the deflection of elevator (δE), and engine throttle setting (δT). Longitudinal control is governed through pitch rate (Q) and consequently angular acceleration ($\dot{\Theta}$) about y-axis (or rate of pitch rate). Longitudinal control of an aircraft is achieved by providing an incremental lift force on horizontal tail. Thus, elevator which is classified as a primary control surface is considered as a pitch control device. The incremental tail lift can be generated by deflecting the entire tail or by deflecting elevator which is located at the tail trailing edge. Since the horizontal tail is located at some distance from the aircraft center of gravity, the incremental lift force creates a pitching moment about the aircraft cg. Pitch control can be achieved by changing the lift on either aft horizontal tail or canard. There are two groups of requirements in the aircraft longitudinal controllability: 1. Pilot force, 2. Aircraft response to the pilot input. In order to deflect the elevator, the pilot must apply a force to stick/yoke/wheel and hold it (in the case of an aircraft with a stick-fixed control system). In an aircraft with a stick-free control system, the pilot force is amplified through such devices as tab and spring. In a conventional symmetric aircraft, the longitudinal control is not coupled with the lateral-directional control. Thus, the design of the elevator is almost entirely independent of the design of the aileron and the rudder. This issue simplifies the design of the elevator. In the design of the elevator, four parameters should be determined. They are: 1) elevator planform area (SE), 2) elevator chord (CE), 3) elevator span (bE), and 4) maximum elevator deflection ($\pm\delta E_{max}$). As a general guidance, the typical values for these parameters are as follows: $SE/Sh = 0.15$ to 0.4 , $bE/bh = 0.8-1$, $CE/Ch = 0.2-0.4$, and $\delta E_{max_up} = -25$ degrees, $\delta E_{max_down} = +20$ degrees. Figure 1 shows the geometry of the horizontal tail and elevator. As a convention, the up deflection of elevator is denoted negative, and down deflection as positive. Thus a, negative elevator deflection is creating a negative horizontal tail lift while generating a positive (nose up) pitching moment.



Top-view of the horizontal tail and elevator

Figure 1. Horizontal tail and elevator geometry

Prior to the design of elevator, the wing and horizontal tail must be designed, as well as the most aft and most forward locations of aircraft center of gravity must be known. In this section, principals of elevator design, design procedure, governing equations, constraints, and design steps as well as a fully solved example are presented.

1.4 Aft Tail Configuration

Aft tail has several configurations that all are able to satisfy the design configurations. Each has unique advantages and disadvantages. The purpose of this section is to provide a comparison between these configurations to enable an aircraft designer to make decision and to select the best one. The aft tail configurations are as follows: 1. Conventional, 2. T-shape, 3. Cruciform (+), 4. H-shape, 5. Triple-tail, 6. V-tail, 7. Inverted V-tail, 8. Improved V-tail 9. Y-tail, 10. Twin vertical tail, 11. Boom-mounted, 12. Inverted boom-mounted, 13. Ring-shape, 14. Twin T, 15. half T, 16. U-tail. Figure 6.10 provides several aft tail configurations.

1.4.1 Conventional

The conventional tail or inverted T-shape configuration (see figure 6.10-1) is the simplest configuration and the most convenient to perform all tail functions (i.e. trim, stability, and control). The analysis and evaluation of the performance of a conventional tail is straight forward. This configuration includes one horizontal tail (two left and right sections); located on the aft fuselage; and one vertical tail (one section); located on top of the aft fuselage. Both horizontal and vertical tails are located and mounted to the aft of fuselage. The horizontal tail is mainly employed to satisfy the longitudinal trim and stability requirements, while vertical tail is mainly used to satisfy the directional trim and stability requirements. If the designer has low experience, it is recommended to initially select the conventional tail configuration. Almost all flight dynamics textbook examine the features of a conventional tail, but not every flight dynamics textbook discuss the characteristics of other tail configurations. The designer must be professional and skillful on the area of the trim analysis, stability analysis, and control analysis, if other configurations are selected. This is one of the reasons that about 60 percent of current aircraft in service have conventional tail. Furthermore it has light weight, efficient, and performs at regular flight conditions.

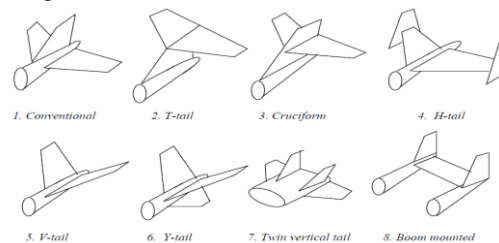


Figure 2. Several aft tail configurations

1.4.2 T-tail

A T-tail is an aft tail configuration (see figure 2-2) that looks like the letter “T”; which implies the vertical tail is located on top of the horizontal tail. The T-tail configuration is another aft tail configuration that provides a few advantages, while it has a few disadvantages. The major advantage of a T-tail configuration is that it is out of the regions of wing wake, wing downwash, wing vortices, and engine exit flow (i.e. hot and turbulent high speed gas). This allows the horizontal tail to provide a higher efficiency, and a safer structure. The lower influence from the wing results in a smaller horizontal tail area; and the lower effect from the engine leads in a less tail vibration and buffet. The less tail vibration increases the life of the tail with a lower fatigue

problem. Furthermore, another advantage of the T-tail is the positive influence of horizontal tail on the vertical tail. It is referred to as the end-plate effect and results in a smaller vertical tail area.

In contrast, the disadvantages that associated with a T-tail are: 1. heavier vertical tail structure, 2. deep stall. The bending moment created by the horizontal tail must be transferred to the fuselage through the vertical tail. This structural behavior requires the vertical tail main spar to be stronger; which cause the vertical tail to get heavier.

Aircraft with T-tail are subject to a dangerous condition known as the deep stall [7]; which is a stalled condition at an angle of attack far above the original stall angle. T-tail Aircraft often suffer a sever pitching moment instability at angles well above the initial stall angle of about 13 degrees, without wing leading edge high lift device, or about 18 degrees, with wing leading edge high lift device. If the pilot allows the aircraft to enter to this unstable region, it might rapidly pitch up to a higher angle of about 40 degrees. The causes of the instability are fuselage vortices, shed from the forward portion of the fuselage at high angles of attack, and the wing and engine wakes. Thus the horizontal tail contribution on the longitudinal stability is largely reduced. Eventually, at a higher angle of attack, the horizontal tail exits the wing and nacelle wakes and the aircraft become longitudinally stable (see figure 3).

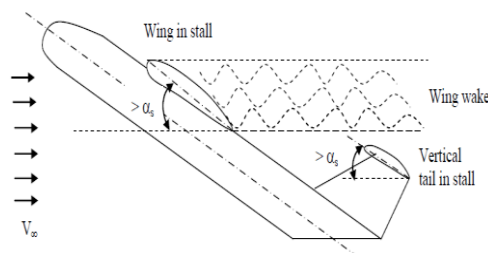


Figure 3. Deep stall in a T-tail configuration aircraft

This condition may be assumed as a stable condition, but it accompanies an enormous drag along with a resulting high rate of descent. At this moment, the elevator and aileron effectiveness have been severely reduced because both wing and horizontal tail are stalled at the very high angle of attack. This is known as a locked-in deep stall, a potentially fatal state. The design solutions to avoid a deep stall in a T-tail configuration are to: 1. Ensure a stable pitch down at the initial stall, 2. Extend the horizontal tail span substantially beyond the nacelles, and 3. Employ a mechanism to enable full down elevator angles if a deep stall occurs. In addition, the aircraft must be well protected from the initial stall by devices such as stick shaker, lights, and stall horn.



Figure 4. Several aircraft with various aft tail configurations

Despite above mentioned disadvantages of T-tail, it becomes more and popular among aircraft designers. About 25 percent of today's aircraft employ T-tail configuration. It is interesting to note that the GA aircraft Piper Cherokee has two versions; Cherokee III with conventional tail, and Cherokee IV with T-tail. The aircraft has a single piston engine at the nose and a low wing configuration. Several GA and transport aircraft such as GrobStarto 2C, Cessna 525 CitaionJet, Beech Super King Air B200, Beechjet T-1A Jayhawk, Learjet 60, Gulfstream IV (Figure 11.15), MD-90, Boeing 727, Fokker 100, AVRO RJ115, Bombardier BD 701 Global

Express, Dassault Falcon 900 (Figure 4-3), Sky Arrow 1450L (see Figure 4-2), Embraer EMB-120, Airbus A400M, and Boeing (formerly McDonnell Douglas) C-17 Globemaster III employ T-tail configuration.

1.4.3 Cruciform

Some tail designers have combined the advantages of conventional tail and T-tail and came up with a new configuration known as cruciform (see figure 2-3). Thus, the disadvantages of both configurations are considerably released. The cruciform; as the name implies; is a combination of horizontal tail and vertical tail such that it looks like a cross or “+” sign. This means that the horizontal tail is installed at almost the middle of the vertical tail. The location of the horizontal tail (i.e. its height relative to the fuselage) must be carefully determined such that the deep stall does not occur and at the same time, the vertical tail does not get too heavy. Several aircraft such as Thurston TA16, Dassault Falcon 2000, ATR 42-400, Dassault Falcon 900B (see figure 4-3), Jetstream 41, Hawker 100, Mirage 2000D employ the cruciform tail configuration.

1.4.4 H-tail

The H-tail (see figure 2-4), as the name implies, looks like the letter “H”. H-tail comprised of one horizontal tail in between two vertical tails. The features associated with an H-tail are as follows:

1. At high angles of attack, the vertical tail is not influenced by the turbulent flow coming from fuselage.
2. In a multiengine turboprop aircraft, vertical tails are located behind the prop-wash region. This causes the vertical tail to have higher performance in the inoperative engine situation.
3. The vertical tail end-plate effect improves the aerodynamic performance of the horizontal tail.
4. In military aircraft, the engine very hot exhaust gasses could be hidden from radars or infrared missiles. This technique has been employed the close support aircraft Fairchild A-10 Thunderbolt (see figure 4-4).
5. The H-tail allows the twin vertical tail span to be shorter. The aircraft “*Lockheed constellation*” had to employ an H-tail configuration to be able to park inside short height hangars.
6. The lateral control of the aircraft will be improved due to the shorter vertical tail span.
7. The H-tail allows the fuselage to be shorter, since the tail can be installed on a boom.
8. The H-tail is slightly heavier than conventional; and T-tail configuration. The reason is that the horizontal tail must be strong enough to support both vertical tails.
9. The structural design of the H-tail is more tedious than conventional tail.

As can be noticed, an H-tail configuration tends to offer several advantages and disadvantages; hence, the selection of an H-tail must be the result of a compromise process. Several GA and military aircraft such as Sadler A-22 Piranha, T-46, Short Skyvan, and Fairchild A-10 Thunderbolt (see figure 4-4) utilize H-tail configuration.

1.4.5 V-tail

When the major goal of the tail design is to reduce the total tail area, the V-tail (see figure 2-5) is a proper candidate. As the name implies, the V-tail configuration has two sections, which forms a shape that looks like the letter “V”. In another word, a V-tail is similar to a horizontal tail with high anhedral angle and without any vertical tail. Two sections of a V-tail act as both horizontal and vertical tails. Due to the angle of each section, the lift perpendicular to each section has two components; one in the y-direction, and one in the z-direction. If no controller is deflected, two components in the y-direction cancel each other, while two lift components in the z-direction are added together. The V-tail may perform the longitudinal and directional trim role satisfactorily, but it has deficiencies in maintaining the aircraft longitudinal and directional stability. In addition, the V-tail design is more susceptible to Dutch roll tendencies than a conventional tail, and total reduction in drag is minimal.

The V-tail design utilizes two slanted tail surfaces to perform the same functions as the surfaces of a conventional elevator and rudder configuration. The movable surfaces, which are usually called ruddervator, are connected through a special linkage that allows the control wheel to move both surfaces simultaneously. On the other hand, displacement of the rudder pedals moves the surfaces differentially, thereby providing directional control. When both rudder and elevator controls are moved by the pilot, a control mixing mechanism moves each surface the appropriate amount. The control system for the V-tail is more complex than that required for a conventional tail. Ruddervator induce the undesirable phenomenon of the adverse roll-yaw coupling. The solution could be an inverted V-tail configuration that has other disadvantages. Few aircraft such as Beechcraft Bonanza V35, Robin ATL Club, Aviation Farm J5 Marco, high-altitude, long-endurance unmanned aerial reconnaissance vehicle Global Hawk (see figure 4-5), and Lockheed F-117 Nighthawk employ a V-tail. Unmanned aircraft General Atomic MQ-1 Predator has an inverted V-tail plus a vertical tail under the aft fuselage.

1.4.6 Y-tail

The Y-tail (see figure 2-6) is an extension to the V-tail, since it has an extra surface located under the aft fuselage. This extra surface reduces the tail contribution in the aircraft dihedral effect. The lower section plays the role of vertical tail, while the two upper sections play the role of the horizontal tail. Therefore, the lower surface has rudder, and the control surface of the upper section plays the role of the elevator. Thus, the complexity of the Y-tail is much lower than the V-tail. One of the reasons this tail configuration is used is to keep the tail out of effect of the wing wake at high angles of attack. The lower section may limit the performance of the aircraft during take-off and landing, since the tail hitting the ground must be avoided. This configuration is not popular, and few old aircraft had this configuration. Unmanned aircraft General Atomic MQ-9 Reaper (see figure 4-6) employ Y-tail configuration.

1.4.7 Twin vertical tail

A twin vertical tail configuration (see figure 2-7) has a regular horizontal tail, but two separate and often parallel vertical tails. The twin vertical tail largely improves the directional controllability of an aircraft. Two short span vertical tails have smaller mass moment of inertia about the x-axis, compared with a long span vertical tail. Thus a twin tail has the same directional control power, while it has a less negative effect of the roll control. In addition, both rudders are almost out of the fuselage wake region, since they are not located along fuselage center line. A disadvantage of this configuration is that they have slightly heavier weight compared with the conventional tail. Several modern fighter aircraft such as F-14 Phantom , McDonnell Douglas F-15 Eagle , and F/A-18 Hornet employ the twin tail configuration.

1.4.8 Boom-mounted

Sometime some specific design requirements do not allow the aircraft designer to select the conventional tail configuration. For instance, if a prop-driven engine must be installed at the rear of the fuselage, a conventional tail will tend to have a low efficiency. The reason is the interference between the propeller flow and the tail. One of the options is to use two booms and install the tail at the end of the booms (see figure 2-8). This option in turn, allows using a shorter fuselage, but overall aircraft weight would be slightly heavier. Two options are: 1. U-tail, 2. Inverted U-tail. The reconnaissance aircraft Reims F337F Super Skymaster (Figure 4-8) and Rutan Voyager employs a boom mounted U-tail. The twin turboprop light utility aircraft Partenavia PD.90 Tapete Air Truck employs a boom mounted inverted U tail configuration which allows for an integrated loading ramp/air-stair.

1.4.9 Other configurations

There is variety of other unconventional tail configurations which are usually the forced options to a designer. For instance, sometimes some specific mission requirements such as loading, operational, structural, and engine requirements removes the conventional or T-tail configuration from the list of possible options. Thus, the designer must come up with a new configuration to make an aircraft trimmed and stable throughout flight. Few invented unconventional configurations are as follows: 1. Boom mounted twin vertical tails plus canard (e.g. Rutan Voyager), 2. Boom mounted twin vertical tails plus two separated horizontal tail (e.g. Space Ship One (figure 4-9)), 3. Twin T-tail (e.g. Global Flyer (figure 4-9)), 4.T-tail plus two fins and an auxiliary fixed horizontal tail (e.g. Beech 1900 D of Continental Express), 5. Ring tail (e.g. Cagny 2000), and 6. Triple vertical tail.

II. LITERATURE SURVEY

2.1 AERODYNAMIC CFD ANALYSIS ON HIGH-LIFT MULTI-ELEMENT WING OF AIRBUS A380:

High-lift systems have a major influence on the sizing, economics, and safety of most transport airplane configurations. Even a small increase in high-lift system performance can make a big difference in the profitability of the aircraft. The added mechanical complexity due to high-lift systems tends to reduce increased payload benefits because of added weight and maintenance costs. A better understanding of high lift flows is needed to continue increasing the performance of high-lift systems while decreasing their complexity. The present work deals with aerodynamic analysis on Airbus A380 high-lift wing system, containing multi-element airfoil with trailing edge flap and leading edge slat. Three flight phases viz., takeoff, cruising and landing are analyzed in both 2D and 3D for lift and drag coefficients. CFD Analysis using ANSYS LUENT 14.0 are performed at various angles of attack, flap angles and slat positions. Effect of flap and slat on lift and drag coefficients on A380 are quantified. During landing, effect of spoilers on lift and drag coefficients are also studied.

Conclusions

- 1) When flap is lowered, it increases the effective angle of attack and generates increased lift. The effect of flap on the CL curve is to offset it in vertical direction. Lowering flap reduces critical angle of attack.
- 2) The effect of slat is to increase the critical angle of attack. Thus an aircraft with slat can take off at very high AOA without losing lift.
- 3) During landing, opening slat reduces lift and hence slat should be opened.
- 4) When spoiler is used, lift becomes highly negative and drag becomes large which is desirable in landing.

2.2 DETERMINATION OF AERODYNAMIC CHARACTERISTICS OF A LIGHT AIRCRAFT USING VISCOUS CFD MODELING

The CFD calculations with included viscous effects represent the latest analyses, aimed for the assessment of aerodynamic characteristics of a new light airplane. During the evolution of such an aircraft, appropriate calculation methods should be applied at the different design development stages. The general trend is application of fairly simple, but reliable analytical and semi-empirical methods at the initial stages, combined with simplified - inviscid CFD computational models, and complex viscous CFD analyses at its final design levels. At the present stage of light aviation development, it is assumed that the contemporary design tools for each of those steps should be appropriate enough, so that they actually verify and additionally fine-tune each other's results. Here presented viscous CFD calculations have been based on the application of unstructured meshes with reasonably small number of elements, combined with robust physical model, involving RANS k- ϵ SST turbulence treatment, which has enabled analyses at around-critical and post-stall angles of attack. These calculations have provided very useful, both quantitative and qualitative aerodynamic data, while the results for aerodynamic coefficients have shown fair agreements with those obtained by methods at previous design levels.

Conclusion

Aerodynamic analyses presented in this paper have been performed using a CFD method which takes into account viscous, but also compressibility effects (no matter how small in case of light aircraft). The calculation model uses mesh with a reasonably small number of elements, and a very sophisticated physical model, based on the RANS k- ϵ SST equations for turbulence. By this, and applying the half-model analysis, the CPU time for calculations of different angles of attack had been substantially reduced, while the range of angles of attack had been extended to the post-stall values, compared with methods applied at previous design steps. Calculations have provided a vast scope of very useful quantitative and qualitative data. Results obtained by all methods during the aerodynamic development of NLA, including the latest CFD calculations, have shown fair agreements for practical engineering purposes. This way, the requirement posted in contemporary airplane design, that the calculation tools and methods applied at all different design levels should generally confirm, supplement and fine-tune each-other, has been satisfied.

2.3 AERO-STRUCTURAL DESIGN AND ANALYSIS OF AN UNMANNED AERIAL VEHICLE AND ITS MISSION ADAPTIVE WING

This thesis investigates the effects of camber change on the mission adaptive wing of a structurally designed unmanned aerial vehicle (UAV). The commercial computational fluid dynamics (CFD) software ANSYS/FLUENT is employed for the aerodynamic analyses. Several cambered airfoils are compared in terms of their aerodynamic coefficients and the effects of the camber change formed in specific sections of the wing on the spanwise pressure distribution are investigated. The mission adaptive wing is modeled structurally to observe the effect of spanwise pressure distribution on the wing structure. For the structural design and analysis of the UAV under this study, commercial software MSC/PATRAN and MSC/NASTRAN are used. The structural static and dynamic analyses of the unmanned aerial vehicle are also performed under specified flight conditions. The results of these analyses show that the designed structure is safe within the flight envelope. Having completed aero-structural design and analysis, the designed unmanned aerial vehicle is manufactured by TUSAŞ Aerospace Industries (TAI).

Conclusion

In the scope of this thesis, the research aiming to increase the aerodynamic efficiency of the aerial vehicles is examined. Among different alternatives, the methodology of increasing the aerodynamic efficiency is chosen as change in camber. The background of the study is established by performing 2D CFD analyses on differently cambered airfoils generated from the selected NACA4412 airfoil via ANSYS®/FLUENT software.

III. UTILIZATION OF TOOLS

3.1 Introduction to CATIA v5

3.1.1 Description about Software

This CATIA project is a direct application of your solid modeling knowledge and skill to a very practical problem to develop an assembly model of a device. Traditionally 2D drafting is highly developed in its ability to convey the geometry of simple 3D parts and solid models represent a straightforward extension. However, solid models can be highly effective when employed to develop complex assemblies of parts into a mechanism or a machine of some kind. When 3D parts can be combined and constrained with a variety of rotating, sliding, twisting, etc. joints, this allows a designer to quickly and accurately explore a greater number of design concepts that can be done without CAD.

CATIA (Computer aided three dimensional interactive application) is a multi-platform CAD/CAM/CAE commercial software suite developed by the French company Dassault and marketed worldwide by IBM. Written in the C++ programming language, CATIA is the cornerstone of the Dassault's mirage fighter jet, and then was adopted in the aerospace, automotive, shipbuilding, and other industries.

3.1.2 History

CATIA started as in-house development by French aircraft manufacturer Avions marcel Dassault, at that time customer of the CAD CAM CAD software.

Initially named CATI (conception assisted tri dimensionally interactive – French for Interactive Aided Three Dimensional Design) – it was renamed CATIA in 1981, when Dassault created a subsidiary to develop and sell the software, and signed to a non-exclusive distribution agreement with IBM. In 1984, All automotive companies use CATIA for car structures-door beams, IP supports, bumper beams, roof rails, body components – because CATIA is very good in surface creation and computer representation of surface
CATIA is widely used throughout the engineering industry, especially in the automotive and aerospace sectors.
CATIA V4, CATIA V5.

3.1.3. Automotive:

Automotive companies that use CATIA to varying degrees are BMW, Porsche, Daimler Chrysler [2], Audi, Volkswagen, Volvo, Fiat, Gestamp automocion, Benteler AG, PSA Peugeot citroen, Renault, Toyota, Honda, Ford, scania, Hyundai, protan, Tata motors and Mahindra. Goodyear uses it in making tires for automotive and aerospace and also uses a customized CATIA for its design and development. All automotive companies use CATIA for car structures-door beams, IP supports, bumper beams, roof rails, body components – because CATIA is very good in surface creation and computer representation of surfaces.

3.1.4. Shipbuilding:

Dassaults system has begun serving shipbuilders with CATIA V5 release 8, which includes special features useful to shipbuilders. GD electric Boat used CATIA to design the latest fast attack submarine class for the United States Navy, the Virginia class. Northrop Grumman Newport news also used CATIA to design the general R. Ford class of supercarriers for the US navy.

3.1.5. Basic part design:

This section will cover the basic use of the part design workbench to create parts. This section will consist of three parts: basic shapes, operations on shapes and interfacing part design sketcher.

Basic shapes:

This part will discuss the various shapes that can be created in part design using the icons on the part design workbench. The purpose of this group of exercises is to introduce how to use those icons and their options. The usefulness of them, depend on the part you are typing to create. It is important for you to understand how to use each of those icons in conjunction with your sketches to produce your final part

Pad: The pad icon allows you to use a sketch and extrude it in a linear direction producing a solid pad. You can create a sketch or profile on-the-fly by pressing the third mouse button while in the selection box. When you create a pad, a pad Definition window appears like the one shown below

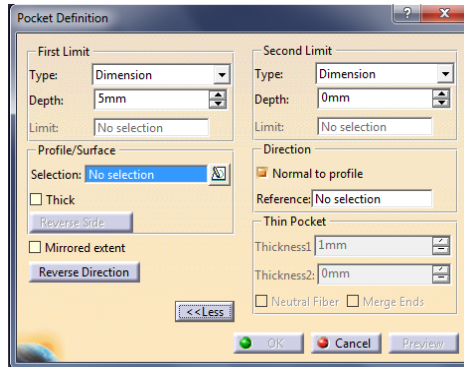


Figure 5 Pad Definition

Pocket:The pocket icon allows you to use a sketch and extrude it in a linear direction producing a pocket.you can create a sketch or profile on the fly by pressing the third mouse button while in the selection box .when you create a pocket , apocket definition window appears like the one shown below

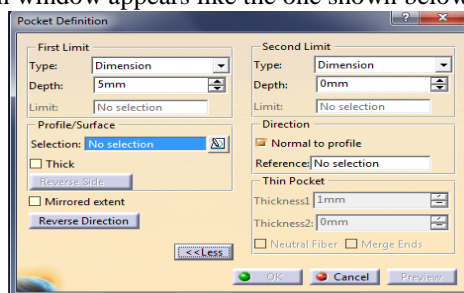


Figure 6 Pocket Definition

3.2. Introduction to ANSYS 12.0

The ANSYS computer program is a large-scale multi-purpose finite element program, which may be used for solving several classes of engineering analyses. The analysis capabilities of ANSYS include the ability to solve static and dynamic structural analyses, steady-state and transient heat transfer problems, mode-frequency and buckling, Eigen value problems, static or time-varying magnetic analyses and various types of field and coupled-field applications. The program contains many special feature which allow nonlinearities or secondary effects to be included in the solution, such as plasticity, large strain hyper elasticity, creep, swelling, large deflections, contact, stress stiffening, temperature dependency, material anisotropy and radiation. ANSYS has been developed, other special capabilities, such as sub structuring, sub modeling, random vibration, kinetostatic, free convention fluid analysis, acoustics, magnetic, piezo electrics, coupled-field analysis and optimization have been added to the program. These capabilities contribute further to making ANSYS a multi-purpose analysis tool for varied engineering disciplines.

The ANSYS program has been in commercial use since 1970, and has been used extensively in the aerospace, automotive, construction, electronics, energy services, manufacturing, nuclear, plastics, oil and steel industries. In addition, many consulting firms and hundreds of universities use ANSYS for analysis, research and educational use. ANSYS is recognized worldwide as one of the most widely used and capable programs of its type.

The ANSYS element library contains more than sixty elements for static and dynamic analyses, over twenty for heat transfer analyses, and includes numerous magnetic, field, and special purpose elements. This variety of elements allows the ANSYS program to analyze two- and three-dimensional frame structures, piping systems, two-dimensional plane and axi-symmetric solids, three-dimensional solids, flat plates, axis- symmetric and three-dimensional shells and nonlinear problems including contacts (interfaces) and cables.

The input data for an ANSYS analysis are prepared using a pre-processor. The general pre-processor (PREP7) contains powerful solid modelling and mesh generation capabilities and is also used to define all other analysis data (geometric properties (real constants), material properties, constraints, loads, etc), with the benefit of database definition and manipulation of analysis data. Parametric input, user files, macros and extensive online documentation are also available, providing more tools and flexibility for the analyst to define the problem. Extensive capability is available throughout the ANSYS program, including isometric, perspective, section, edge and hidden-line displays of three-dimensional structures, x-y graphs of input quantities and result and contour displays of solution results. a graphical user interface is available throughout the program, to guide new users through the learning process and provide more experienced users with multiple windows, pull-down

menus, dialog boxes, tools bar and online documentation.

The analysis results are reviewed using postprocessors, which have the ability to display distorted geometries, stress and strain contours, flow fields, safety factor contours, contours of potential field results (thermal, electric, magnetic), vector field displays, mode shapes and time history graphs. The postprocessors can also be used for algebraic operations that may be performed on seismic modal results. Response spectra may be generated from dynamic analysis results from various loading modes that may be combined for harmonically loaded axisymmetric structures.

The main purpose of the project shall be to determine the structural parameters such as total deformation, equivalent stresses which is also known as Von-Mises stress. The modal analysis will be carried out to find out the first 4 modes of vibrations and the different mode shapes in which the wing can deform without the application of load. The outcomes and shortcomings, if any, will be analyzed and suitable mitigation measures will be presented.

Different types of analysis carried out are:

1. Modal analysis
2. Structural analysis
3. Gravity analysis
4. Transient analysis

IV. MODELING OF DESIGN

4.1 ELEVATOR MODELING

In the process of analysis the first step is to model the problem. For this, we have used some of the available software's.

4.1.1 CATIA V5

CATIA (Computer Aided Three-dimensional Interactive Application) is a multi-platform CAD/CAM/CAE commercial software suite developed by the French company Dassault Systems. Written in the C++ programming language, CATIA is the cornerstone of the Dassault Systems product lifecycle management software suite. The key points generated by using MACROS are then imported into the CATIA. Using these key points the required airfoils and wing are generated. The generated wing must be saved in .iges format for its further use in ANSYS workbench.

CATIA V5 PART

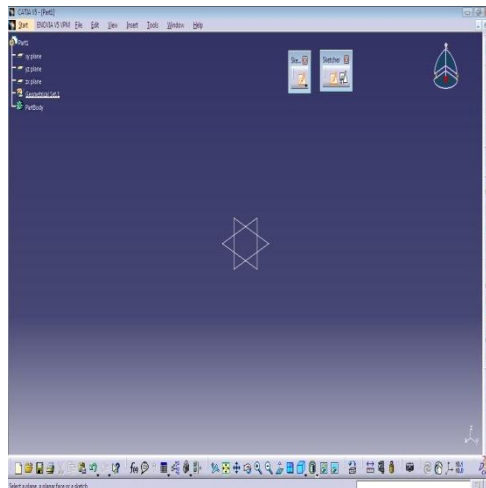


Figure 7 Catia part

The "Part" workbench provides a set of functionalities for creating and modifying 3D solid elements. It is a feature-based, parametric solid modeling design workbench. You can create fully associative 3D solid models, with or without constraints.

Part Toolbars

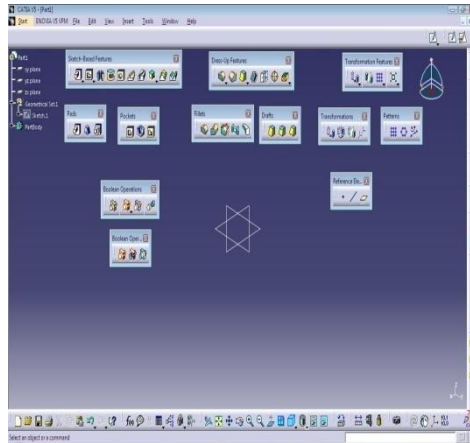


Figure 8 Part Tool bar

Features can be classified as sketch-based or dress-up:

- Sketch-based features are created using a 2D sketch. Generally, the sketch is transformed into a 3D solid by extruding, rotating, sweeping, or lofting.
- Dress-up features are created directly on the solid model. Fillets and chamfers are examples of this type of feature.

A CATIA document is made up of individual elements. These elements are called *features*. While creating a document, you can add features such as pads, pockets, holes, ribs, fillets, chamfers, and drafts. As the features are created, they are applied directly to the work piece.

CATIA graphically displays the feature-based structure and other non-graphical data of your model in the form of a *specification tree*. The specification tree shows the sequence in which the features were created, and enables you to easily access all the underlying associated information and elements.



The Sketch-Based features toolbar is available in extended or compact display mode. To choose your display mode, use the View -> Toolbars -> Sketch-Based Feature (Extended/Compact) command.

Specifications

➤ Area (m ²)	=	31.00
➤ Span (m)	=	12.45
➤ Aspect Ratio	=	5.00
➤ Taper Ratio	=	0.256
➤ 1/4 Chord Sweep (°)	=	29.00
➤ Tail Arm (m)	=	13.53
➤ Sh/S	=	0.253
➤ ShLh/Sc	=	0.799

4.2 NACA 0009 AIRFOIL DATA

NACA-0009 9.0% smoothed

1.00000 0.0
 0.99572 0.00057
 0.98296 0.00218
 0.96194 0.00463
 0.93301 0.00770
 0.89668 0.01127
 0.85355 0.01522
 0.80438 0.01945
 0.75000 0.02384
 0.69134 0.02823
 0.62941 0.03247

0.56526 0.03638
0.50000 0.03978
0.43474 0.04248
0.37059 0.04431
0.33928 0.04484
0.30866 0.04509
0.27886 0.04504
0.25000 0.04466
0.22221 0.04397
0.19562 0.04295
0.17033 0.04161
0.14645 0.03994
0.12408 0.03795
0.10332 0.03564
0.08427 0.03305
0.06699 0.03023
0.05156 0.02720
0.03806 0.02395
0.02653 0.02039
0.01704 0.01646
0.00961 0.01214
0.00428 0.00767
0.00107 0.00349
0.0 0.0
0.00107 -0.00349
0.00428 -0.00767
0.00961 -0.01214
0.01704 -0.01646
0.02653 -0.02039
0.03806 -0.02395
0.05156 -0.02720
0.06699 -0.03023
0.08427 -0.03305
0.10332 -0.03564
0.12408 -0.03795
0.14645 -0.03994
0.17033 -0.04161
0.19562 -0.04295
0.22221 -0.04397
0.25000 -0.04466
0.27886 -0.04504
0.30866 -0.04509
0.33928 -0.04484
0.37059 -0.04431
0.43474 -0.04248
0.50000 -0.03978
0.56526 -0.03638
0.62941 -0.03247
0.69134 -0.02823
0.75000 -0.02384
0.80438 -0.01945
0.85355 -0.01522
0.89668 -0.01127
0.93301 -0.00770
0.96194 -0.00463
0.98296 -0.00218
0.99572 -0.00057
1.00000 0.0

4.3 TOTAL DESIGN OF HORIZONTAL STABILIZER AND ELEVATOR

- The NACA 0009 airfoil co-ordinates are imported into the CATIA V5.
- By using spline tool the points are joined so that the correct airfoil shape is going to obtain.
- By using extrude tool bar the airfoil surface has been extruded.
- The trim is performed for elevator design.
- The below figure shows the design of horizontal stabilizer.

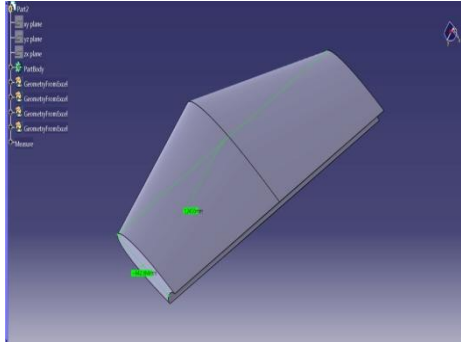


Figure 9 Horizontal stabilizer

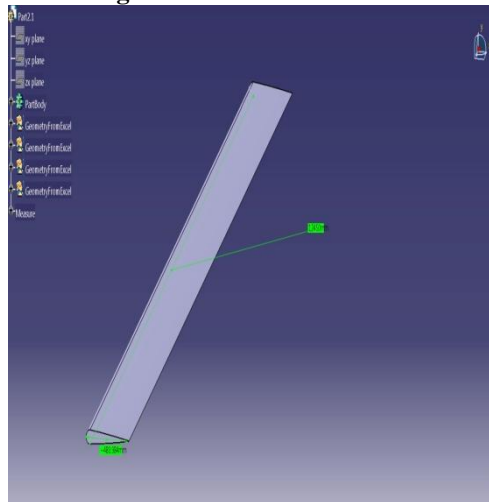


Figure 10 Elevator

The above figure shows the top view, side view and front view.

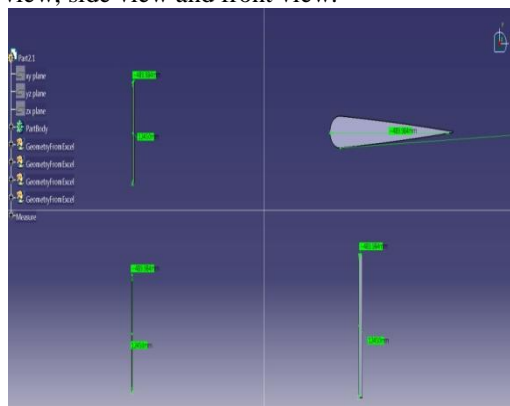


Figure 11 Total design of horizontal stabilizer and elevator

V. COMPUTATIONAL ANALYSIS OF DESIGN :

5.1 INTRODUCTION TO CFD

In the present work an attempt has been made to study the aerodynamic characteristics of NACA 0009 aerofoil using CFD and comparing the results with Prandtl-glauert law. Hence there is a need to know about the fundamentals of computational fluid dynamics before venturing in to the actual problem. In this chapter a brief introduction and explanation about computational fluid dynamics is outlined.

5.1.1 WHAT IS CFD?

“CFD is the science of predicting fluid flow, heat and mass transfer, chemical reactions and related phenomenon by solving numerically the set of governing mathematical equations”

Computational fluid dynamics is the analysis of system involving fluid flow, heat transfer and associated phenomena such as chemical reactions by means of computer-based simulation. The technique is very powerful and spans a wide range of industrial and non-industrial applications areas. Some examples are aerodynamics of aircrafts and vehicles, hydrodynamics of ships, combustions, turbo machinery, electrical and electronic engineering, chemical process engineering, external and internal environment of buildings, marine engineering, and biomedical engineering etc. from the 1960s onwards, the aerospace industry has integrated CFD technique into design, R&D and manufacture of aircraft and jet engines. More recently the methods have been applied to the design of internal conduction engines, combustion chambers of gas turbines and furnaces. Furthermore, motor vehicles manufacturers now routinely predict drag forces, under-bonnet airflow and the in-car environment with CFD. Increasingly CFD is becoming a vital component in the design of industrial products and processes.

The ultimate aim of development in the CFD field is to provide a capability Comparable to other CAE (Computer-Aided-Engineering) tools such as stress analysis codes. This remains as the reason why CFD has lagged behind is the tremendous complexity of the underlying behaviour, which precludes a description of the fluid flow this is at the same time economical and sufficiently complete. The availability of affordable high performance computing hardware and introduction of the user-friendly interface has led to a recent upsurge of interest and CFD is poised to make an empty into the wider industrial community in the 1990s. Clearly the investment costs of a CFD capability are not small, but the total expense is not normally as great as that of a high quality experimental facility. Moreover, there are several unique advantages of CFD over experimental-based approaches to fluid.

SYSTEMS DESIGN:

- Substantial reduction of lead times and costs of new designs
- Ability to study systems where controlled experiments are difficult or impossible to perform(e.g. very large systems)
- Ability to study the systems under hazardous conditions at and beyond their normal performance limits(e.g. safety studies and accident scenarios)
- Practical unlimited level of detail of results.

In contrast CFD codes can produce extremely large volumes of results at virtually no added expense and it is very cheap to perform parametric studies, for instance to optimize equipment performance.

5.2. HOW DOES CFD CODE WORK

CFD codes are structured around the numerical algorithms that can tackle fluid flow problems. In order to provide easy access to their solving power all commercial CFD packages include sophisticated user interfaces to input problem parameters and to examine the results.

Hence all codes contain three main elements:

- (1) Pre-processor
- (2) Solver
- (3) Post- processor

Computational method

The NACA 0009, the well documented aerofoil from the 4-digit series of NACA aerofoils, was utilized. The NACA 0009 aerofoil is symmetrical; the 00 indicates that it has no camber. The 09 indicates that the aerofoil has a 09% thickness to chord length ratio; it is 09% as thick as it is long. Reynolds number for the simulations was $Re=3 \times 10^6$, same with the reliable experimental data from Abbott and Von Doenhoff (1959), in order to validate the present simulation. The free stream temperature is 300 K, which is the same as the environmental temperature. The density of the air at the given temperature is $\rho=1.225 \text{ kg/m}^3$ and the viscosity is $\mu=1.7894 \times 10^{-5} \text{ kg/ms}$. For this Reynolds number, the flow can be described as incompressible. This is an assumption close to reality and it is not necessary to resolve the energy equation. A segregated, implicit solver was utilized (Fluent Gambit 6.3.26., 2006) Calculations were done for angles of attack ranging from -12 to 20° . The airfoil profile, boundary conditions and meshes were all created in the pre-processor Gambit 2.4.6. The pre-processor is a program that can be employed to produce models in two and three dimensions, using structured or unstructured meshes, which can consist of a variety of elements, such as quadrilateral, triangular or tetrahedral elements. The resolution of the mesh was greater in regions where greater computational accuracy was needed, such as the region close to the airfoil.

The first step in performing a CFD simulation should be to investigate the effect of the mesh size on the solution results. Generally, a numerical solution becomes more accurate as more nodes are used, but using additional nodes also increases the required computer memory and computational time. The appropriate number of nodes can be determined by increasing the number of nodes until the mesh is sufficiently fine so that further refinement does not change the results. This study revealed that a C-type grid topology with 80000 quadrilateral cells would be sufficient to establish a grid independent solution. The domain height was set to approximately 20 chord lengths and the height of the first cell adjacent to the surface was set to 10^{-5} , corresponding to a maximum y^+ of approximately 0.2. A y^+ of this size should be sufficient to properly resolve the inner parts of the boundary layer

In order to include the transition effects in the aerodynamic coefficients calculation and get accurate results for the drag coefficient, a new method was used. The transition point from laminar to turbulent flow on the airfoil was determined and the computational mesh was split in two regions, a laminar and a turbulent region. To calculate the transition point the following procedure was used. A random value for the transition point (x_{tr}) was chosen and the computational domain was split at that point with a perpendicular line. The problem was simulated in Fluent after defining the left region as laminar and the right as turbulent zone.

5.3. FLOW ANALYSIS:

We Considered air flowing over NACA 0009 airfoil with elevator deflection at different angles. The freestream velocity is 80 m/s. Assume standard sea-level values for the freestream properties:

Pressure = 101,325 Pa

Density = 1.2250 kg/m³

Temperature = 288.16 K

Kinematic viscosity $\nu = 1.4607 \times 10^{-5}$ m²/s

We will determine the lift and drag coefficients under these conditions using FLUENT.

Step 1: Create Geometry in CATIA V5

Main Menu > File > Import .

Click on the enclosure tool to get the box. For **File Name**, browse and select the elevator.stp file. Select both **Vertices** and **Edges** under **Geometry to Create**: since these are the geometric entities we need to create.

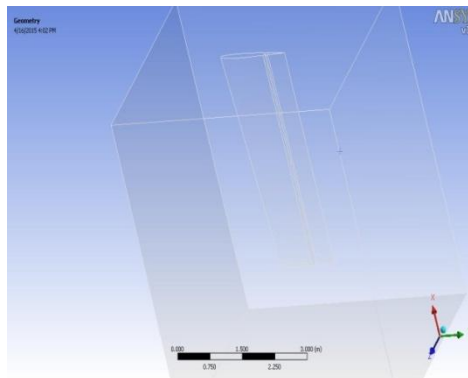


Figure 12 Geometry with enclosure

Step 2: Mesh Geometry

Mesh Faces

We'll mesh each of the 3 faces separately to get our final mesh. Before we mesh a face, we need to define the point distribution for each of the edges that form the face i.e. we first have to mesh the edges. We'll select the mesh stretching parameters and number of divisions for each edge based on three criteria:

1. We'd like to cluster points near the airfoil since this is where the flow is modified the most; the mesh resolution as we approach the farfield boundaries can become progressively coarser since the flow gradients approach zero.
2. Close to the surface, we need the most resolution near the leading and trailing edges since these are critical areas with the steepest gradients.
3. We want transitions in mesh size to be smooth; large, discontinuous changes in the mesh size significantly decrease the numerical accuracy

Mesh the face. The resultant mesh is shown below.

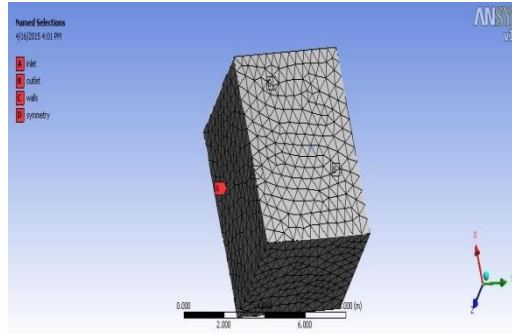


Figure 13 Mesh Geometry

VI. RESULTS AND DISCUSSION

Obtained numerical results can generally be divided into “global” and “detailed”, where the most important global assessments imply the lift coefficient C_L , drag coefficient C_D and pitching moment coefficient C_M with elevator at three characteristic positions.

α [°]	C_M	C_L
-8	-0.012	-0.555
0	-0.001	0.001
5	-0.042	0.752
20	-0.111	0.854
25	-0.134	0.912
30	-0.155	0.632

Table 1 C_L, C_M Coefficients @ 5°

α [°]	C_M	C_L
-8	-0.023	-0.611
0	-0.003	0.211
5	-0.042	1.000
20	-0.031	1.122
25	-0.054	1.422
30	-0.145	1.895

Table 2 C_L, C_M Coefficients @ 10°

α [°]	C_M	C_L
-8	-0.074	-1.000
0	0.033	0.231
5	0.052	0.451
20	0.011	0.622
25	0.021	0.844
30	-0.052	1.112

Table 3 C_L, C_M Coefficients @ -10°

Presented results, obtained by CFD analyses, show moderate increase in maximum lift coefficient with elevator deflection.

The CFD aerodynamic analyses have been performed for angles of attack α [°] ranging from negative, to positive post-stall values, at Reynolds number $MRe \approx 5.3$ calculated with respect to the wing chord, for all elevator positions (to retain full compatibility of the results, although such MRe value would be a bit too high for operational elevator applications). The analyses have provided very useful quantitative and qualitative results.

VII. CONCLUSION

Aerodynamic analyses presented in this paper have been performed using a CFD method which takes into account viscous, but also compressibility effects. The calculation model uses mesh with a reasonably small number of elements, and a very sophisticated physical model, based on the RANS k- ω SST equations for turbulence. By this, and applying the half-model analysis, the CPU time for calculations of different angles of attack had been substantially reduced, Results obtained by all methods during the aerodynamic development of

NLA, including the latest CFD calculations, have shown fair agreements for practical engineering purposes. This way, the requirement posted in contemporary airplane design, that the calculation tools and methods applied at all different design levels should generally confirm, supplement and fine-tune each-other, has been satisfied. For this study, several software packages were used independently to create and obtain an optimal elevator design. The specific packages used include CATIAV5 and FLUENT 12.1. Through flow analysis we specify Lift and Drag convergence history of symmetrical airfoil elevator and pressure distribution and velocity distribution results are plotted.

REFERENCES

- [1]. Longitudinal control characteristics of a 1/10-scale model of the Convair F-102 airplane at transonic speeds By Robert S. Osborne and Kenneth E. Tempelmeyer, Langley Aeronautical Laboratory, Langley Field, Va.
- [2]. R.C. Nelson: Flight Stability and Automatic Control (second edition), McGraw-Hill, 1998
- [3]. Ajoy Kumar Kundu: Aircraft Design, Cambridge University Press, 2010
- [4]. Valarezo WO., Dominik CJ., McGhee RJ., Goodman WL., Paschal KB., Multi-Element Airfoil
- [5]. Optimization for Maximum Lift at High Reynolds Numbers, AIAA Paper 91-3332, Sept. 1991.
- [6]. Valarezo WO., Dominik CJ., McGhee RJ., Reynolds and Mach Number Effects on Multi-element Airfoils, in Proceedings of the Fifth Numerical and Physical Aspects of Aerodynamic Flows, California State University, Long Beach, CA, Jan. 1992.
- [7]. van Dam CP., The aerodynamic design of multi-element high-lift systems for transport airplanes, Progress in Aerospace Sciences, Vol 38, pp 101-144, 2002.
- [8]. Daniel Reckzeh, Airbus Aerodynamic Design & Data Domain Germany, Aerodynamic Design of Airbus High-Lift Wings in Multidisciplinary Environment, European Congress on Computational Methods in Applied Sciences and Engineering (ECCOMAS 2004), Jyväskylä, 24—28 July 2004.
- [9]. Reckzeh D., CFD-Methods for the Design Process of High-Lift Configurations (11th AG-STAB –DGLR Symposium 1998), New Results on Numerical and Experimental Fluid Mechanics Volume 72, pp 347-354, Vieweg Verlag, 1999
- [10]. Bertin, J., Smith, M. (1989). Aerodynamics for engineers, Prentice - Hall International Editions, ISBN: 0-13-018227-3, Englewood Cliffs, NJ
- [11]. ANSYS FLUENT 14.0 (2011): Theory Guide, ANSYS, Inc., Canonsburg, PA
- [12]. ANSYS FLUENT 14.0 (2011): User's Guide, ANSYS, Inc., Canonsburg, PA
- [13]. ANSYS FLUENT 14.0 (2011): Tutorial Guide, ANSYS, Inc., Canonsburg, PA